Formation of hill and valley structures on Si(001) vicinal surfaces studied by spot-profile-analyzing LEED

H. Minoda,* T. Shimakura, and K. Yagi
Department of Physics, Tokyo Institute of Technology, Oh-okayama, Meguro, Tokyo 152-8551, Japan

F.-J. Meyer zu Heringdorf and M. Horn von Hoegen
Institut für Festkörperphysik, Universität of Hannover, Appelstrasse 2, D-30167 Hannover, Germany
(Received 22 June 1999; revised manuscript received 27 September 1999)

Formation of ''hill-and-valley'' structures on Si(001) vicinal surfaces induced by Au adsorption which accompanies formation of the Si(001)5×3.2-Au reconstruction, was studied by *in situ* high-resolution low-energy electron diffraction. The ''hill-and-valley'' structures are composed of (001) terraces and (119) facets under the equilibrium condition independent of the miscut angle (0.5–8°) of the substrate surfaces. This does not depend on sample treatments and the similar structures are obtained by annealing after Au deposition at room temperature as well as Au deposition at high temperature. *In situ* observation during annealing indicates that commensurate fivefold structures such as 5×3 and $\sqrt{26}\times3$ that were previously observed are not formed on the Si(001) surface and only the 5×3.2 structure is formed in this system. Double domain structures initially formed in such a way that the 5×3.2 and 3.2×5 domains are formed on the 2×1 and 1×2 terraces, respectively, finally transforms into single domain 5×3.2 structure where the fivefold direction is parallel to the miscut direction.

I. INTRODUCTION

Clean Si(001) vicinal surfaces inclined toward the $[1\bar{1}0]$ direction exhibit two kinds of domain and step structure depending on the miscut angle.[1–3] Vicinal surfaces with small miscut angles have double domain structure composed of 2×1 and 1×2 domains. They are arranged alternately along the miscut direction and are separated by single height steps (S_A- and S_B-type steps). On the other hand, 2×1 domains cover most of the vicinal surfaces for large miscut angles (>5°) and the dimer bond direction of the majority domain is perpendicular to the miscut direction and neighboring terraces are separated by *B*-type double height steps (D_B steps).

Metal adsorption on Si(001) modifies surface reconstructions that depend on substrate temperature, adsorbate metal and its coverage and modifies the surface energy and its anisotropy. Most metals grow in the Stranski-Krastanov mode on the Si(001), i.e., metal adsorption on the Si(001) causes a reduction of the surface free energy. Thus, metal adsorption on Si(001) vicinal surface would causes changes in step configuration and Si(001) terraces with metal adsorption expand due to changes in surface free energy. At the same time step bunching occurs because the areas where surface steps are accumulated should be formed to conserve the macroscopic orientation.

Several studies of metal adsorption-induced step bunching and faceting have been performed.[4–16] Recently, we have been studied Au adsorption-induced faceting on a Si(001) 4° off vicinal surface[13,16] and found that deposition of Au at temperatures above 750 °C drastically modifies surface morphology. The vicinal surface forms a ''hill-and-valley'' structure composed of (001) terraces and facets. The facet orientations depend on the deposition conditions. Only (119) facets are formed above 850 °C. (117) and (115) facets are formed below 850 °C in addition to the (119) facets. Real time observations of the surface morphology change during Au deposition show that the faceting processes are proceeds in four stages.[14]

During faceting processes changes in domain structure are observed and single-domain structure of the 4° off surface initially changes into double domain structure and it finally changes into the single domain structure with the 5×3.2 reconstruction. Electron microscope observations during Au deposition reveal a large anisotropy in the growth speed of the 5×3.2 domains and the growth speed perpendicular to the fivefold directions is two orders of magnitude faster than that parallel to the five-fold direction. In the present paper miscut angle and substrate temperature dependence of a ''hill-and-valley'' structure after faceting studied by spot profile analyzing low-energy electron diffraction (SPA-LEED) are described. Changes in domain structures by annealing after Au deposition at room temperature are also presented.

II. EXPERIMENT

The experiments were performed in a standard ultrahigh vacuum (UHV) chamber with base pressure of 1×10^{-8} Pa equipped with a SPA-LEED system and an evaporator for Au. Si samples were cut from Si(001) wafers with miscut angles of 0.5°, 4°, and 8° towards the $[1\bar{1}0]$ direction. After degassing at 650 °C for 24 h the samples were flash heated to 1200 °C to remove the native oxide. Au was deposited at a deposition rate of about 0.1 ML/min at temperatures between 770 and 870 °C. Some of the Au films were annealed after Au deposition at room temperature.

The SPA-LEED system has two incident electron guns. One with normal incidence was used to obtain standard two-dimensional LEED patterns. One-dimensional LEED pat-

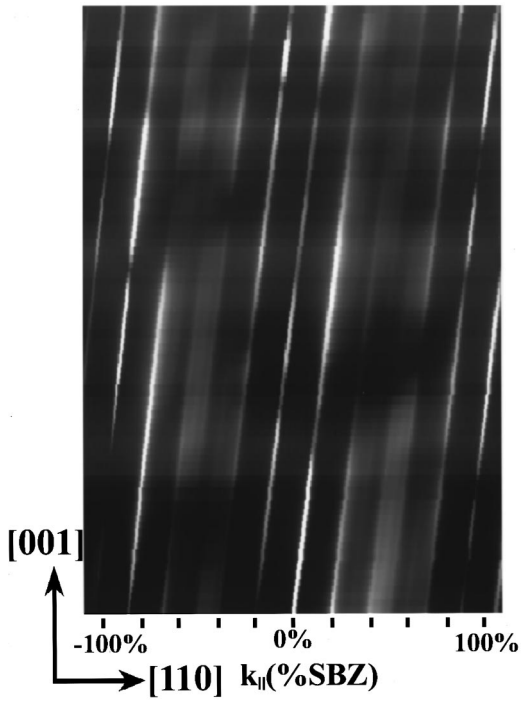

FIG. 1. A vertical cut in reciprocal space of a clean Si(001) 8° off vicinal surface with $k_{\parallel}$ as the x axis and $k_{\perp}$ as the y axis. Right hand side is the [110] direction and vertical direction is the [001].

terns (or 1D LEED patterns) were monitored during Au deposition using a second electron gun in a grazing incidence geometry.[17] This allows investigation of the kinetics of the morphological transformation during Au adsorption. 1D LEED patterns at various electron energies were taken after quenching to room temperature to construct a vertical cut in reciprocal space of surfaces with $k_{\parallel}$ as the x (the miscut direction) axis and $k_{\perp}$ as the y axis.

III. RESULTS AND DISCUSSION

A. High-temperature Au deposition

The surface morphology of the initial surface before Au deposition could be deduced from Fig. 1. The morphology could be investigated from the variation of surface rod positions in reciprocal space as a function of the vertical scattering vector. Figure 1 shows a vertical cut in reciprocal space of the initial Si(001) 8° off vicinal surface (an 8° off surface) with $k_{\parallel}$ as the x axis along the $[1\bar{1}0]$ direction and $k_{\perp}$ as the y axis in the [001] direction. Measured intensities are plotted in a logarithmic and a gray-scale representation in Fig. 1. This vertical cut of reciprocal space was constructed as follows. The 1D LEED patterns along the miscut direction (the [110] direction) through the (00) rod of the (001) surface were measured for various incident electron energies from 82 eV (the second Bragg condition (008) for (001) surface) to 180 eV [the third Bragg condition (0012)], and they are aligned vertically. The width of this figure corresponds to 220% of the surface Brillouin zone (SBZ) of the (001) surface. All bright lines correspond to reciprocal rods from the surface and are inclined by 8° from the vertical (the [001]) direction, showing that the surface is inclined toward [110] direction by 8° from the (001) surface.

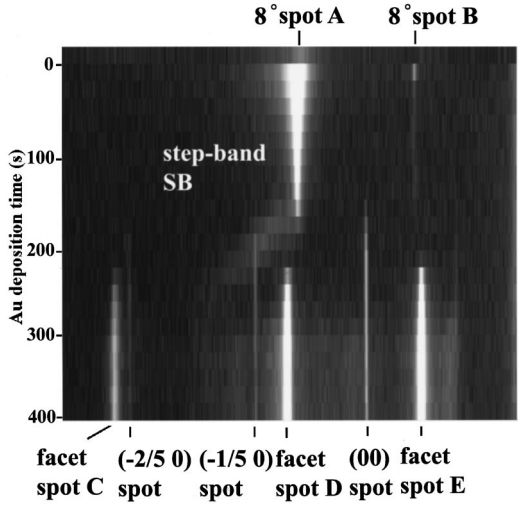

FIG. 2. A change of the 1D LEED pattern during Au deposition at 870 °C.

Au was deposited on the 8° off surface at 870 °C. Changes in surface morphology during Au deposition were investigated by using the second electron gun. The spot profile of the 1D LEED pattern along the [110] direction through the (00) rod of the (001) surface was measured during Au deposition. Changes in the intensity distribution of the 1D LEED pattern are shown in Fig. 2. (Incident electron energy was 110 eV and it is close to the in-phase condition ($S=1.02$).) The x axis shows reciprocal space vector along the $[1\bar{1}0]$ direction and the y axis shows the Au deposition time. Prior to Au deposition LEED spots from the 8° off surface are seen as indicated by *A* and *B*. Changes in surface morphology are similar to that observed during Au deposition on the 4° off surface[14] and four different stages could be distinguished. Stage 1: no change in the surface morphology, stage 2: nucleation of (001)5×3.2 terraces, stage 3: growth of the 5×3.2 terraces and step bunching or step band formation and stage 4: faceting (transformation of the step bands into the facets).

Just after the start of Au deposition facet spots *A* and *B* increase in intensity due to an increase of reflectivity by Au adsorption. After that LEED spots *A* and *B* slightly decrease in intensity but do not move until approximately 150 s. Adsorption of Au on the surface enhances surface diffusion of Si atoms to enhance thermal fluctuation of narrowly spaced steps.[18] This corresponds to an increase in the Debye-Waller factor of the system. In spite of the enhanced thermal fluctuation of the steps the surface morphology does not change until 150 s because the spots *A* and *B* do not move (stage 1). Spots from the 5×3.2 domains on the Si(001) surface appear 150 s after the start of the deposition showing nucleation of the 5×3.2 domains (stage 2). With further Au deposition diffraction intensity from the 5×3.2 domains increases while at the same time a broad spot arising from the step bands (SB) is developing and changing its position. The increased intensity of the 5×3.2 spots corresponds to expansion of the 5×3.2 domains. The movement of the spot SB corresponds to an increase in inclination angle of the step bands (step bunching) (stage 3). Finally, sharp spots *C*-*E* from the facets appear and the spot SB disappears at the same time reflecting the transformation of step bands into facets (stage 4).

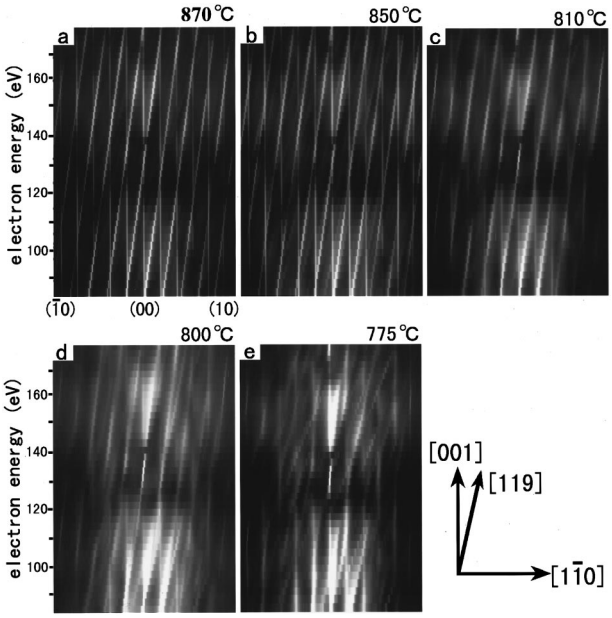

FIG. 3. A temperature dependence of the [110] cross section of a reciprocal space of the (b) 8° off vicinal surface after faceting. Substrate temperatures in (a)–(c) are 870, 850, 815, 800, and 775 °C, respectively. In all the figures vertical lines are from the (001) surfaces.

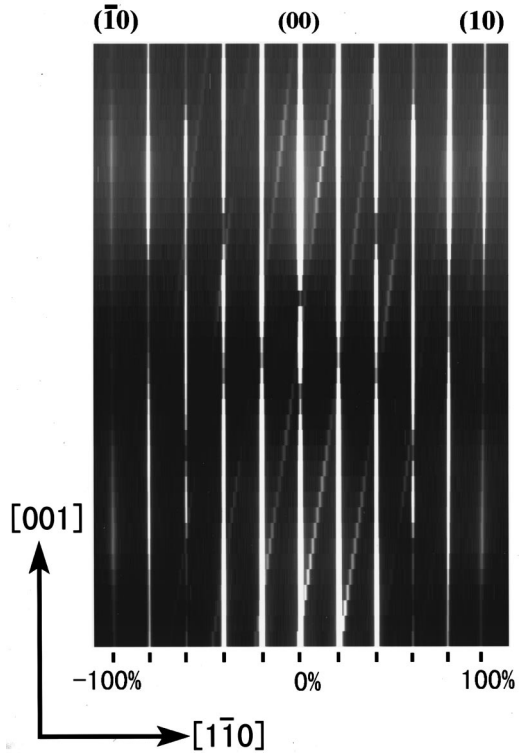

FIG. 4. A vertical cut in reciprocal space of the 0.5° off surface after Au deposition with $k_{\parallel}$ as the x axis and $k_{\perp}$ as the y axis.

Substrate temperature dependence of the facet orientation formed after Au deposition on the 8° off surface was investigated. As in Fig. 1, Figs. 3(a)–3(c) show vertical cuts in reciprocal space of the 8° off surfaces after Au deposition at various substrate temperatures with $k_{\parallel}$ as the x axis and $k_{\perp}$ as the y axis. Substrate temperatures in Figs. 3(a)–3(c) are 870, 850, 815, 800, and 775 °C, respectively. Widths of all the figures correspond to the 220% of SBZ and the center positions of the lower and the upper edges correspond to the (008) and (0012) reciprocal lattice points. Figure 3(a) was obtained after measurement of Fig. 2 and very sharp vertical lines are seen. Distances between neighboring vertical lines correspond to the 20% of SBZ of the (001) surface. The corresponding 2D LEED pattern (not shown) show the formation of the single domain Si(001)5×3.2-Au structure on the (001) terraces. Thus, the vertical lines on the n/5th positions are from the Si(001)5×3.2 structure. In addition to the vertical lines, bright and sharp inclined lines are seen in (a). They are inclined by 8.9° from the (001) surface toward the [110] direction and the formation of (119) facets with 8×2 reconstruction is concluded.[14] Figures 3(b) and 3(c) are similar to Fig. 3(a). However, in Fig. 3(c) the background intensity is higher and the vertical and inclined lines are more diffuse than in Figs. 3(a) and 3(b). Integrated intensities of spots from the (001)5×3.2 areas and the (119) facets decrease with decreasing substrate temperature from Figs. 3(a) to 3(c). These facts mean that areas with the [001] and the [119] orientations formed at lower temperature are smaller. At higher temperature ''hill-and-valley'' structures are well ordered and the surface morphology should get closer to the equilibrium shape. Intensities of vertical lines are lower in Figs. 3(d) and 3(e) and inclined lines, in several orientations with larger inclined angles than those from the (119) facets are seen in Figs. 3(d) and 3(e). Thus, the formation of various kinds of facets at lower temperatures is concluded.

On Si(001) vicinal surfaces with small miscut angles the average step-step distance is large and it is not likely to form facets with definite orientations such as [119] and [117]. However, it was found that even on a 0.5° off surface ''hill-and-valley'' structures composed of (001) and (119) facets were formed. Figure 4 shows a vertical cut in reciprocal space of the 0.5° off surface after Au deposition at 870 °C with $k_{\parallel}$ as the x axis and $k_{\perp}$ as the y axis. The facet rods are quite similar to those in Fig. 3(a). The only difference between Figs. 3(a) and 4 is in relative intensities of the two types of the rods. On the 0.5° off initial surface all surface steps are single height steps and the average step-step distance is approximately 15.6 nm. From real space observations by electron and optical microscopy we know that the typical width of a single (001) terrace with the 5×3.2 structure in a ''hill-and-valley'' structure formed on a 4° off surface is larger than hundreds of nm and is at least one order of magnitude larger than the average step-step distance on the 0.5° off surface. Thus, it is possible that during Au deposition several tens of steps can bunch together to form step bands which transform into facets.

Figure 5 shows the intensity of the facet spot relative to that of the (00) spot of the (001) terraces as a function of the miscut angle of the sample. Open circles show experimental values and all the data were obtained after Au deposition at about 870 °C. At 870 °C kinetic effects are (i) negligible[16] and a ''hill-and-valley'' structure obtained after Au deposition is considered to be the (ii) equilibrium structure. Filled circles show calculated ratios of the projected areas of the facets to the (001) plane. Both behaviors are quite similar to each other and the experimental values are approximately

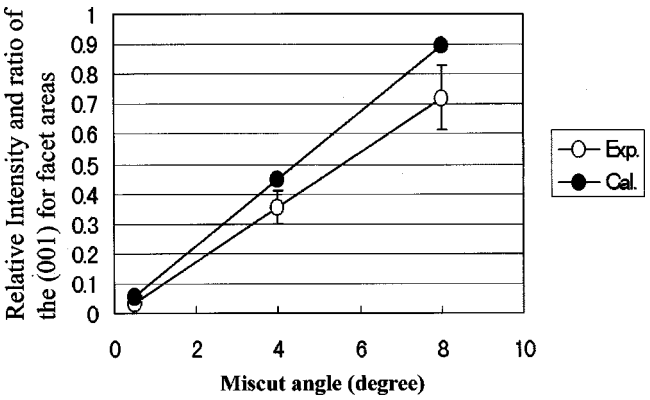

FIG. 5. An intensity of the facet spot relative to the (00) spot as a function of miscut angle of the sample. Samples were obtained by Au deposition at 870 °C. Open circles show experimental values and close circles show calculated ratios of the projected areas of the (119) facets to the (001) plane.

80% of the calculated values. Assuming that the reflectivity of the facet spot is approximately 80% for the (00) reflection of the (001) surface we can conclude that the (001) and the (119) facets cover the entire surface.

From our observations that ''hill-and-valley'' structures composed of (001) and (119) facets are formed on three different substrate orientation we can conclude that they are the most stable structures on Si(001) vicinal surfaces with miscut angle below 8.9°. This suggests that the following relationship between the surface free energies of the $(001)5\times3.2$-Au and that of the $(119)8\times2$-Au holds.

$$\gamma(119)\cos 8.9° < \gamma(001)$$

$$\text{or} \quad \gamma(001)\cos 8.9° < \gamma(119).$$

Thus,

$$0.988\gamma(001) < \gamma(119) < 1.012\gamma(001).$$

The two surfaces have similar surface energies and the difference is approximately 1%.

Our previous observation during annealing after high-temperature Au deposition seems to show that Au $\gamma(001) < \gamma(119)$ because the (119) facets vanish before the $(001)5\times3.2$ areas do so during annealing.[14] Another notable thing is that the (001) facets grow faster than (119) facet during annealing after Au deposition on a 8° off surface at room temperature (RT) in spite of the fact that larger mass transport is necessary to form the (001) facets on the 8° off surface than the (119) facets (see Fig. 6).

Thus,

$$\gamma(001) < \gamma(119) < 1.012\gamma(001).$$

B. Annealing after Au deposition at room temperature

In the previous section Au adsorption-induced faceting on the Si(001) vicinal surfaces during high-temperature Au deposition have been described. In this section, changes in the surface morphology and domain structures during annealing after Au deposition at room temperature are described. Faceting also occurs when samples are annealed after several ML's of Au deposition at room temperature.

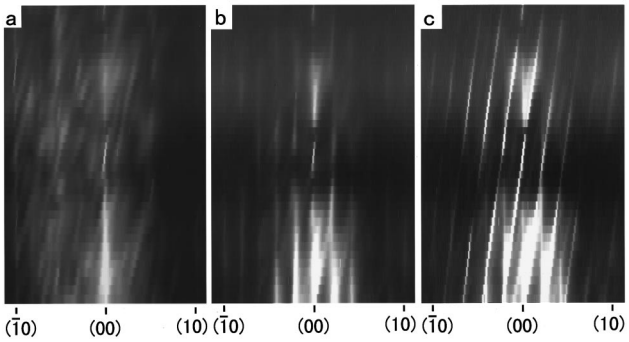

FIG. 6. Vertical cuts in reciprocal space of the 8° off surfaces at various annealing with $k_{\parallel}$ as the x axis and $k_{\perp}$ as the y axis. Annealing temperatures of (a)–(c) are 770, 825, and 890 °C, respectively.

Figures 6(a)–6(b) show vertical cut in reciprocal space of the 8° off surfaces at various annealing temperatures with $k_{\parallel}$ as the x axis, which is parallel top the miscut direction and $k_{\perp}$ as the y axis. Annealing temperatures of Figs. 6(a)–6(c) are 770, 825, and 890 °C, respectively. The central vertical line in each image corresponds to the (00) rod of the (001) surface. Diffuse rods inclined from the vertical direction are seen in Fig. 6(a) and are due to the Au-covered initial 8° off surface. In Fig. 6(b), relatively sharp rods from the five-fold structure are seen and part of the surface is known to be covered by (001) terraces with the 5×3.2 structure. Very weak inclined rods are due to formation of small facets. The fact that rod from the (001) facet is stronger than that from the inclined facet suggests that (001) facet is the most stable facets around this area. Thus, $\gamma(001)$ would be lower than $\gamma(119)$. The inclined rods become stronger and sharper at 890 °C as in (c) indicating that the facet areas grow larger. Vertical lines also become sharper in Fig. 6(c) showing the formation of a ''hill-and-valley'' structure composed of (001) terraces and (119) facets. Comparing with Fig. 3, spots form the (001) and the (119) facets are more diffuse in Fig. 6(c). This is explained by smaller sizes of (001) terraces in Fig. 6(c) due to large miscut.

Changes in the surface morphology are induced by the formation of the 5×3.2 structure and change of its domain structure. The change in the domain structure during annealing has been studied by continuous measurements of the 1D LEED patterns during annealing and shown in Fig. 7 at 85 eV electron energy during the heating process. The intensity in the directions parallel and perpendicular to the miscut directions through the (00) rod of the (001) surface were measured alternately and are shown in Figs. 7(a) and 7(b), respectively. Several MI's of Au were deposited on the 0.5° off surface at room temperature and the sample was heated up to 700 °C and the measurement of the intensity distributions was started after that. Sharp vertical lines at the center in both panels correspond to the (00) rods. The width of the both panels is 220% of SBZ for the (001) surface. Strong vertical lines at the right and left sides in Fig. 7(a) correspond to the (10) and (−10) spots and in Fig. 7(b) to the (01) and (0–1) spots. With increasing substrate temperature intensity distributions in Figs. 7(a) and 7(b) change because the surface morphology as well as the surface reconstruction changes. At the initial stage at 700 °C, strong peaks are seen

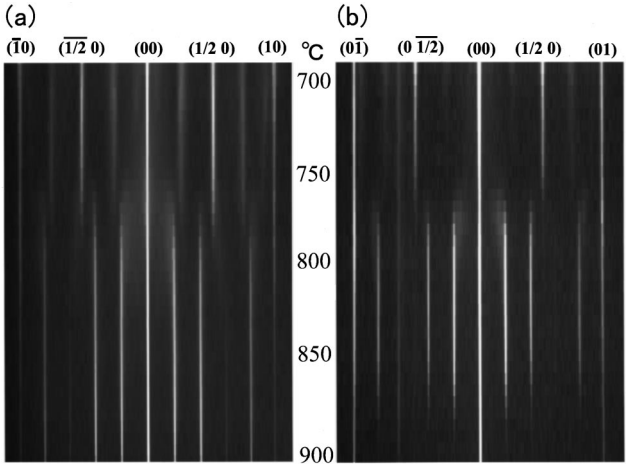

FIG. 7. Intensity distribution of 1D LEED patterns in the directions (a) parallel and (b) perpendicular to the miscut direction through the (00) rod of the (001) surface during the annealing process. More than 1 ML of Au was deposited on the 0.5° off surface at RT and the sample was heated up to 700 °C and the measurement of the intensity distributions were started.

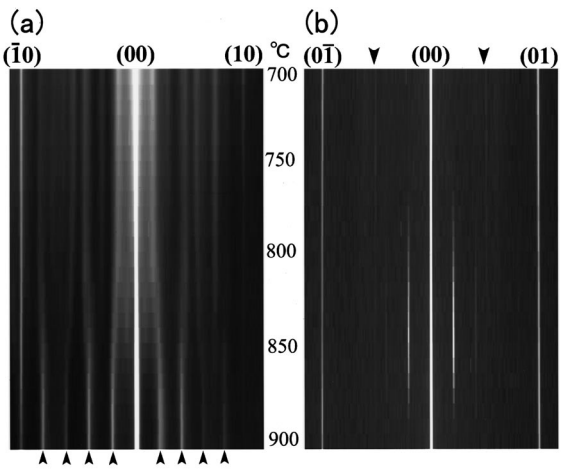

FIG. 8. Intensity distribution of the 1D LEED patterns in the directions (a) parallel and (b) perpendicular to the miscut direction through the (00) rod of the (001) surface during the annealing process. More than 1 ML of Au was deposited on the 4° off surface at RT and the sample was heated up to 700 °C and the measurement of the intensity distributions were started.

at the half-order positions in each panel. At this temperature a $c(2\times8)$ structure is formed on the (001) terraces and corresponding spots are seen at the $n/4$th order positions with stronger intensities in Fig. 7(a) than in Fig. 7(b). Intensity distributions in the both panels change drastically at 770 °C. The $c(2\times8)$ spots decrease in intensity and new spots appear at $n/5$th order positions in Figs. 7(a) and 7(b). The $c(2\times8)$ structure transforms into a fivefold structure. It is noted that spots from a three-fold structure are observed in both panels. This does not mean that commensurate threefold structures as reported previously[19–21] such as 5×3 or $\sqrt{26}\times3$ structures are formed on this surface. Only a structure denoted as the 5×3.2 structure is observed in 2D LEED patterns by annealing after Au deposition at room temperature. We conclude that the $c(2\times8)$ structure transforms into the 5×3.2 structure at about 770 °C and the 5×3.2 structure is only the structure observed by diffraction methods above 770 °C in the present study. Recently, an scanning tunneling microscopy (STM) study showed that the 5×3.2 structure is composed of the 5×3 and the $\sqrt{26}\times3$ units and quasiperiodicity with five unit cells of $3a_0$ period gives rise to the 3.2-fold periodicity.[22]

The superlattice spots from the fivefold structure appear at the same temperatures in Figs. 7(a) and 7(b). This means that the 5×3.2 domains with two orientations nucleate at the same temperature at about 770 °C. The spots from the 5×3.2 structure in (a) remain up to more than 900 °C, while those in Fig. 7(b) disappear at about 880 °C and a single domain 5×3.2 structure is formed.

Using samples with 4° and 8° miscut surfaces, similar experiments as in Fig. 7 were performed and qualitatively similar changes in the intensity distributions are observed. Figures 8(a) and 8(b) show changes in the intensity distributions in the directions parallel and perpendicular to the miscut direction, respectively, through the (00) rod of the (001) surface during annealing after Au deposition on the 4° off surface. Before Au deposition the single domain structure characteristic to large miscut is formed and *B* terraces where twofold direction of the domains is perpendicular to the miscut direction (2×1 domains) are dominant. After annealing up to 700 °C the 2×1 structure transforms into the $c(2\times8)$ structure and the eightfold direction of the $c(2\times8)$ structure is parallel to the twofold direction of the 2×1 structure. Thus, spots at half order positions indicated by arrowheads in Fig. 8(b) are considered to be from the $c(2\times8)$ structure. In this figure, intensities of the spots from the $c(2\times8)$ structure are much lower than that in Fig. 7. In Fig. 8 total areas with the $c(2\times8)$ structure and their domain size will be much smaller than those in Fig. 6 because inclination angle of the surface in Fig. 8 is larger than that in Fig. 7. In spite that the intensity distribution in Fig. 8(a) is much complicated due to formation of rough surface, many spots are seen. The spots at the half-order positions from $c(2\times8)$ domains are not seen in Fig. 8(a) showing that the $c(2\times8)$ structure is in a single orientation. At about 770 °C spots from the fivefold structure especially at the $(0\pm1/5)$ positions appear only in Fig. 8(b). As described before the $c(2\times8)$ structure transforms into the 5×3.2 structure and this indicates that the fivefold direction of the 5×3.2 structure is parallel to the eightfold direction of the $c(2\times8)$ structure and to the twofold direction of the clean Si(001)2×1 structure.

Spots from the fivefold structure indicated by arrow heads appears around 850 °C in Fig. 8(a) showing that nucleation of the 5×3.2 domains starts at this temperature. The spots from the 5×3.2 domains in Fig. 8(a) as well as those in Fig. 8(b) increase in intensity with increasing substrate temperature. However, the intensities in Fig. 8(b) decrease and the spots from the fivefold structure disappear at 880 °C. This suggests that the 3.2×5 domains re-arrange into the 5×3.2 domains by annealing and step structure should change drastically during this process. Finally, the spots from the 5×3.2 structure are seen only in Fig. 8(a) indicating that the single domain 5×3.2 structure is formed on the surface as in the case of high temperature deposition. When Au is deposited on the 4° off surface at about 800 °C, a change from a

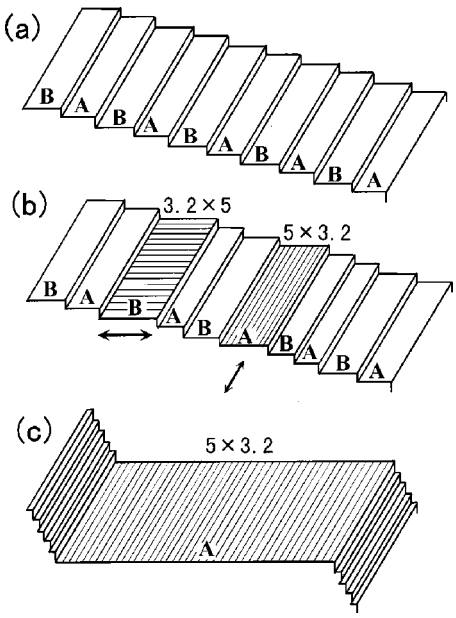

FIG. 9. Schematic diagrams, that show changes of the domain structures after Au deposition followed by annealing. (a) an initial surface, (b) nucleation of the 5×3.2 structure, (c) a final surface.

double domain structure to a single domain structure is observed.[14] Figures 7 and 8 show a similar change in the domain structure during annealing.

Before Au deposition *B*-type terraces cover the entire surface of the 4 and 8° off surfaces and D_B-type steps are the domain boundaries. As described before the 5×3.2 terraces cover the entire surfaces at the final stage and the 5×3.2 domains are formed on the 2×1 *A*-type terraces. These mean that all the surface steps after Au deposition are *A*-type steps with even integer height steps. Thus, Au adsorption is considered to destabilize the D_B-type steps, to separate them into S_A and S_B-type steps at the initial stage and to stabilize D_A-type steps, which accompany growth of the single domain 5×3.2 structure.

During annealing, changes in the surface morphology in Figs. 7 and 8 are not clearly seen as in Fig. 2. This is due to the fact that in the case of annealing, nucleation densities of the 5×3.2 structures are much higher and their sizes are much lower than those in the case of high temperature Au deposition. As shown before (in Fig. 6), the facet rods obtained by annealing is more diffuse than that obtained by high temperature Au deposition in Fig. 3. Another possible explanation of differences between Figs. 7 and 8 and Fig. 2, and between Fig. 6 and Fig. 3 is kinetic effect. Since a ''hill-and-valley'' structure composed of the (001) and (119) facets is the most stable structure, mobility of Si and Au atoms are much higher when Au was deposited at high temperature. The kinetic effect on the surface morphology still exists in deposition below 860 °C. Thus, a ''hill-and-valley'' structure obtained by annealing experiment would not be a complete equilibrium structure probably due to shortage of annealing time.

Schematic diagrams in Fig. 9 show changes in the domain structures during the annealing process on the vicinal surface with a small miscut angle such as 0.5°. In the case of the surface with a small miscut angle $2\times1(A)$ and $1\times2(B)$ terraces exist and the $c(8\times2)$ and $c(2\times8)$ domains nucleate on respective terraces. The $c(8\times2)$ and $c(2\times8)$ domains transform into the 5×3.2 and 3.2×5 domains, respectively at about 770 °C. The 5×3.2 and 3.2×5 domains grow larger by further annealing. Growth speed of the 5×3.2 structure, however, is very anisotropic and the speed perpendicular to the fivefold direction indicated by arrows is much faster than that parallel to the fivefold direction.[14] When a 5×3.2 domain (formed on the *A*-type terrace) grows along the preferential growth direction (perpendicular to the fivefold direction) almost no mass transport of Si is necessary. On the other hand large amount of mass transport of Si is necessary when a 3.2×5 domain grows along the preferential direction because step movement is necessary. Thus, the growth speed of the 3.2×5 domain should be reduced due to mass transport restriction. Nucleation rates of the 5×3.2 and the 3.2×5 domains should be the same. However, the 5×3.2 areas can become larger than 3.2×5 areas due to the different growth rates.

A reason for the transformation from the double domain structure into single-domain structures by high-temperature annealing is as follows. When the 5×3.2 structure is formed, an array of domain boundaries (steps or step bands) are formed on the vicinal surface, because the preferential growth direction of the 5×3.2 domains is perpendicular to the miscut direction and is parallel to the steps on the vicinal surface. On the other hand, growths of the 3.2×5 domains are limited not only along the slow growth direction (perpendicular to the miscut direction) but also along the preferential growth direction (parallel to the miscut direction) due to suppression by surface diffusion of Si atoms as mentioned before. Thus, the surfaces covered mainly by the 3.2×5 domains or two orientational domains are considered to have short segmented. These structures would cost more energy than that covered mainly by the 5×3.2 domains because the formation energy of the domain boundaries is relatively high. (This can be known from the fact that domain boundaries are very straight.[14]) Thus, the 5×3.2 domains would be a lower energy structure and the 3×5.2 domains should transform into the 5×3.2 domains during the growth of the domain structure to reduce the total energy of the system.

For the case of the surface with large miscut angle changes in the domain structure can be explained in the same way as in Fig. 9. However, difference in domain structure at the initial stage should be taken into account. In the case of the surface with large miscut angle, D_B-type step is the most stable steps and 1×2 domains (*B* terraces) cover the entire surface before Au deposition. In this case nucleation rate of the 3.2×5 domains is much higher than that of the 5×3.2 domains at the initial stage of the annealing process. However, there may be 2×1 domains on the surface due to thermal step fluctuation. Si atom density included in the 5×3.2 structure and/or the $c(2\times8)$ structure may differ from that in the Si(001)2×1 structure and a difference may also modify step configuration during annealing. Thus, nucleation of the 5×3.2 domains also occurs on the 2×1 domain. As described before 5×3.2 domains can easily expand and grow larger than the 3.2×5 domains. The 3.2×5 domains should be destroyed by the growth of the 5×3.2 domains and the 5×3.2 domains cover the almost all the surfaces at high temperature.

IV. SUMMARY

Faceting on Si(001) vicinal surfaces induced by Au deposition at high-temperature deposition and annealing (up to 900 °C) after room temperature deposition were studied by *in situ* SPA-LEED. The three facts are commonly observed in two types of experiments on substrate surfaces with inclination angle in a range of 0.5–8° from the (001) orientation toward the [110] direction. (1) ''hill-and-valley'' structure composed of the $(001)5\times3.2$-Au terraces and the $(119)8\times2$-Au facets are formed at high temperatures, which indicates that this structure is the most stable phase in this system. The surface morphology depends on the deposition condition and it gets apart form the equilibrium shape and facets with larger inclination angles are formed at lower substrate temperature. (2) During the growth process of the 5×3.2 structures double domain structures are formed and they transform into the single-domain structures of the 5×3.2 terraces whose fivefold direction is parallel to the miscut direction at the final stage of the growth of the 5×3.2 structure. (3) The previously reported commensurate Au-adsorbed Si(001) structure such as the 5×3 and the $\sqrt{26}\times3$ structure are not formed in either experiments and only the incommensurate 5×3.2 pattern is observed in this system above 770 °C.

From the fact that two facets are thermally stable on varied miscut angle surfaces [fact (1)], relatively large cusps at the [001] and [119] orientations in the γ plot of Au-covered Si surfaces are concluded. The surface free energy of the $(119)8\times2$ surface is almost the same as that of the $(001)5\times3.2$ surface but the $(001)5\times3.2$ facet is more stable than the $(119)8\times2$ facets.

The fact (2) was explained by anisotropy in growth speed of the 5×3.2 domains and high formation energy of the domain boundaries of the 5×3.2 and the 3.2×5 domains or the surface steps. The growth speed perpendicular to the five-fold direction is much faster than that parallel to it. The 5×3.2 domains can easily expand without appreciable mass transport of Si in the direction perpendicular to the fivefold direction, which is perpendicular to the miscut direction. Moreover, total length of the steps should not increase during growth of the 5×3.2 domains. On the other hand, another type of domains (the 3.2×5 domains) cannot expand along the preferential growth direction because large amount of mass transport of Si is necessary in this case. Moreover, growth of the 3.2×5 domains along the preferential growth direction (the miscut direction) increases domain boundary or the surface steps, which increases the total energy of the system. Thus, the surface morphology with the 3.2×5 domains is not energetically favorable. This explanation is common to the two types of the experiments and to various miscut angle surfaces, although there are some differences in detail as discussed in the previous section.

From the comparison of the annealing experiments on the differently oriented vicinal surfaces, relationship of the orientations of the 2×1, the $c(8\times2)$ and the 5×3.2 structures are clarified. The $c(8\times2)$ and the $c(2\times8)$ domains nucleated on the 2×1 and 1×2 terraces, respectively and they transforms into the 5×3.2 and the 3.2×5 domains, respectively. Thus, the two-fold direction of the 2×1 structure is parallel to the fourfold direction of the $c(2\times8)$ structure and to the fivefold direction of the 5×3.2 structure.

ACKNOWLEDGMENTS

Discussions with Professor M. Henzler are gratefully acknowledged. This work was supported by Grant-in Aid from Ministry of Education of Japan (Nos. 07044133 and 09NP1201) and the Deutsche Forschungsgemeinschaft (Ho1611/4-1).

*Author to whom correspondence should be addressed. Electronic address: hminoda@surface.phys.titech.ac.jp

[1] J. Wasserfall and W. Ranke, Surf. Sci. **315**, 227 (1994).
[2] M. Hanbucken, B. Rottger, and H. Neddermyer, Surf. Sci. **331–333**, 1028 (1995).
[3] C. C. Umbach, M. E. Keeffe, and J. M. Blakely, J. Vac. Sci. Technol. B **9**, 721 (1991).
[4] E. Suliga and M. Henzler, J. Vac. Sci. Technol. A **1**, 1507 (1982).
[5] M. Jalochowski, M. Strozak, and R. Zdyb, Surf. Sci. **375**, 203 (1997).
[6] K. Aoki, H. Minoda, Y. Tanishiro, and K. Yagi, Surf. Rev. Lett. **5**, 653 (1998).
[7] K. Aoki, T. Suzuki, H. Minoda, Y. Tanishiro, and K. Yagi, Surf. Sci. **408**, 101 (1998).
[8] P. R. Pukite and P. I. Cohen, Appl. Phys. Lett. **50**, 1739 (1987).
[9] S. Folsch, D. Winau, G. Meyer, K. H. Rieder, M. Horn von Hoegen, T. Schmidt, and M. Henzler, Appl. Phys. Lett. **67**, 2185 (1995).
[10] S. Folsch, G. Meyer, K. H. Rieder, M. Horn von Hoegen, T. Schmidt, and M. Henzler, Surf. Sci. **394**, 60 (1997).
[11] A. Meier, P. Zahl, R. Vockenroth, and M. Horn von Hoegen, Appl. Surf. Sci. **123/124**, 694 (1998).
[12] X.-S. Wang and E. D. Williams, Surf. Sci. **400**, 220 (1998).
[13] M. Horn von Hoegen, H. Minoda, K. Yagi, F.-J. Meyer zu Heringdorf, and D. Kähler, Surf. Sci. **402–404**, 464 (1998).
[14] H. Minoda, K. Yagi, F.-J. Meyer zu Heringdorf, A. Meire, D. Kähler, and M. Horn von Hoegen, Phys. Rev. B **59**, 2363 (1999).
[15] F.-J. Meyer zu Heringdorf, D. Kähler, M. Horn von Hoegen, Th. Schmidt, E. Bauer, M. Copel, and H. Minoda, Surf. Rev. Lett. **5**, 1167 (1998).
[16] H. Minoda and K. Yagi, Surf. Sci. Lett. **437**, 1 (1999).
[17] M. Horn von Hoegen, J. Falta, and M. Henzler, Thin Solid Films **183**, 213 (1989).
[18] T. Shimakura, H. Minoda, Y. Tanishiro, and K. Yagi, Surf. Sci. **407**, L6 (1998).
[19] K. Oura, Y. Makino, and T. Hanawa, Jpn. J. Appl. Phys., Part 1 **15**, 737 (1976).
[20] X. F. Lin, K. J. Wan, J. C. Glueckstein, and J. Nogami, Phys. Rev. B **47**, 3671 (1993).
[21] G. Jayaram and L. Marks, Surf. Rev. Lett. **2**, 731 (1995).
[22] M. Horn von Hoegen, F.-J. Meyer zu Heringdorf, R. Hild, P. Zahl, Th. Schmidt, and E. Bauer, Surf. Sci. **433–435**, 475 (1999).